MINISTERUL EDUCAȚIEI
UNIVERSITATEA TEHNICĂ DIN CLUJ-NAPOCA

Field: Electrical engineering

PhD THESIS

– ABSTRACT –

Development, analysis and testing of a control method based on behavior remodeling of a single-phase AC/DC PWM converter.

PhD Studnet:
Ing. Ionuț Sorin SALCU

PhD Supervisor:
Prof. Dr. Călin Gh. RUSU

Examination Comitee:

Chiar: Prof. Dr. Ing. **Loránd Szabó –** Universitatea Tehnică din Cluj-Napoca;
PhD Supervisor: Prof. Dr. Ing. **Călin Gh. Rusu –** Universitatea Tehnică din Cluj-Napoca;
Members:
- Prof. Dr. Ing. **Petre Lucian Ogruțan –** Universitatea Transilvania din Brașov;
- Prof. Dr. Ing. **Ioan Nașcu –** Universitatea Tehnică din Cluj-Napoca;
- Conf. Dr. Ing. **Ciprian Șorândaru –** Universitatea Politehnica Timișoara.

– Cluj-Napoca –
2023

Contents

INTRODUCTION

The situation of electricity consumption and generation is, already for a long time, a leitmotif related to the optimization and innovation of new technologies. Aspects such as "smart" grids and distributed generation are currently being addressed for widespread deployment. Micro-grids are becoming an integrated part of modern local energy production and storage systems and applications [1], [2]. They can operate in parallel with the "classic" electricity distribution network as individual entities, or in connection with it, allowing the management of the transfer of energy between the two. Typically, microgrids are designed to operate in direct current (DC) or as having multiple voltage levels. For this, dedicated circuit topologies, [3], [4], are studied and proposed to be implemented as solutions. Also, the implementation of low voltage alternating current (AC) systems is treated within this concept [5], [6]. The management of the energy transiting such a network thus becomes a key element in making it more efficient, increasing performance and reducing operating costs. In addition to these, the point of common connection (PCC) with the public power network, or with other similar networks, involves special attention in terms of the quality of electricity [7]–[10].

Since the interaction between the different power modes: in A.C. or in D.C., which characterizes the diversity of the previously mentioned solutions, is mediated by specific converters, they are forced to adopt a behavior that guarantees a minimum energy quality. AC/DC converters have already become essential in powering everyday equipment, but this brings with it a risk to AC networks, which can be exposed to poor performance due to the precarious behavior of these equipment. Although the configurations and control methods of these converters end up meeting the requirements imposed by international regulations, it is often necessary to implement additional structures in the system to mitigate and optimize energy consumption. These equipment usually have a reactive character and role in managing the flow of reactive energy, with the aim of stabilizing the parameters of the AC power supply network [11]–[14]. The shortcoming in this regard may refer to the fact that, in order to increase the performance of the system, it is necessary to introduce additional equipment, which leads to an increase in the overall installed power level, without directly serving the final consumers. This aspect is treated in papers [15], [16]. Within them, the concept is proposed to maintain the level of power initially installed at the PCC of the network, but to assign a secondary electronic function to the AC/DC converters. The latter would thus be able to participate in conditioning the quality of electricity at the PCC, within the limits of the available power reserve or their load level. An elaborate study of this concept can be found in reference [17], with the aim of deepening the research in this direction.

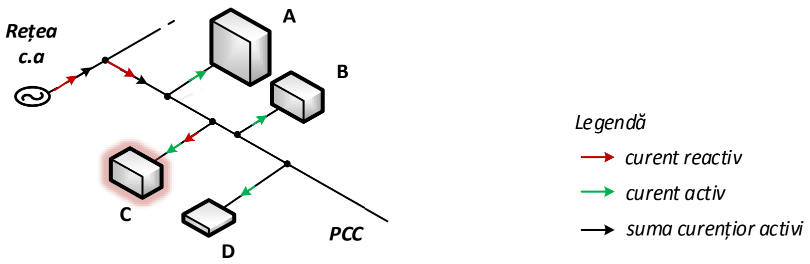

a) C – reactive power consumption la PCC

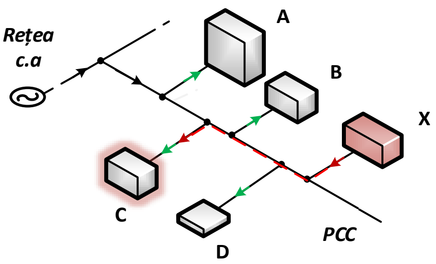

b) X – reactive power compensation

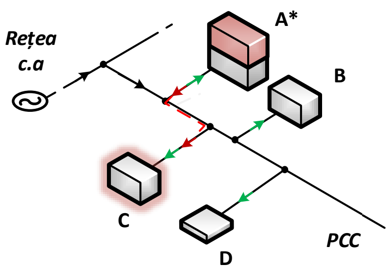

c) A* - taking over the compensation function

Fig. 1 – Representation of the concept of the secondary electronic function of a PCC powered equipment.

An illustration of the mentioned concept is represented in Fig.1 a). Here you can see a series of AC loads, labeled A-D, connected to the PCC of a power supply. It is assumed that one of the consumers, marked "C", has a reactive character. To mitigate its impact on the supply network, in Fig.1 b), the equipment marked "X" has the role of compensating the reactive energy at the PCC. The compensation capacity is set according to its power level. Thus, in the power system, the total installed power is represented by the power of consumers A-D and that of equipment X. Analyzing the representation in Fig.1 c), the problem arises of the situation in which the consumer A would not operate at maximum power, and in addition it would present a bidirectional character at the input, in terms of energy consumption. In this situation, the role of compensating the reactive power content at the PCC could be performed by device A, now denoted "A*", by using the available power reserve at its level. So, by reallocating the existing but unused power, to serve a secondary functionality, it can be stated that the level of total power that is found at a given moment circulating in the system, necessary to obtain the targeted performances, is lower. This would equate to an increase in system-wide power density.

The present thesis wishes to continue the exploration of the reactive power management concept at PCC proposed and discussed in the previously mentioned papers. The purpose of this thesis is to study the behavior of an AC/DC bidirectional converter, its limitations in operation and how a new control method would cause the classic topology of the converter to actively participate in improving the quality of electricity, at the system level, by remodeling its behavior vis-à-vis the AC network. It is also desired to include the expanded concept of "power density" in this context, something argued by the author by the lack of need to introduce additional equipment into the system.

The content of the thesis is structured in six chapters, whose structure is as follows:

Chapter 1 – follows the overview of the topologies currently used to make ac/dc converters. single phase. Both unidirectional and bidirectional structures of these converters will be presented, emphasizing their mode of operation at unity power factor. Also, the main control techniques used in the operation of these converters will be exposed. At the same time, the review of the main current methods applied for synchronization with the supply network, a crucial aspect in controlling the character of the power consumption of the converter, will be presented in this chapter. To conclude, the author proposes a discussion related to the concept of "power density" and how it could be extended to include the core concept of the present paper.

Chapter 2 – the content of this chapter presents the classical mathematical model of the single-phase, controlled, AC/DC converter, with the purpose to study its operation. Also, the state model for the presence of reactive power at the input of the converter will be made, and finally, its integration in the mathematical model, to obtain the general expressions, which correspond to the operation of the AC/DC converter, in any given situation.

Chapter 3 – the observation of the operation of the unitary power factor converter and the implementation of the related control strategy, are exemplified in this chapter. A non-linear control method is also proposed, for cases where the output power of the AC/DC converter varies.

Chapter 4 – follows the implementation of the control strategy, customized to achieve the active compensation of the power factor at the PCC by the converter. Its performance and limitations in adopting this behavior are discussed.

Chapter 5 – the implementation of a real-time simulation, which aims to test and validate the control method addressed to the converter. The obtained results are interpreted.

Chapter 6 – general conclusions and discussions about the aspects found in the content of the work. The author's contribution is emphasized, as well as future perspectives for the development of the treated concept.

2 MATHEMATICAL MODEL OF THE CONVERTER

In this chapter, the modeling of the converter for its operating regimes was addressed. Initially, the representation was made in the form of state equations of its operation for a unitary power factor, thus the entire power circulated at the system level was active power. The stages followed in the realization of the state model and the definition of the transfer functions that correlated the output quantities, i.e. the current through the coil and the capacitor voltage, with the input ones were presented. The supply voltage and the duty cycle of the control signal were considered as inputs.

The particular aspect is characterized by raising the problem of modeling the converter for the states in which it operates on reactive power. After obtaining the model, it was desired to integrate it into the general description of the system's behavior. For this, it was studied how the average power would vary, for sinusoidal input quantities, with the increase of the phase shift. The justification comes in the context where the phase shift between voltage and current directly influences the instantaneous power value. It was concluded that the average power variation depends on the phase shift through a cosine function. Thus, two coefficients were introduced with the aim of weighting the driving states of the converter by the average power level at a given phase shift. Finally, the transfer functions of the system were expressed, including the aspect previously presented.

An electronic AC/DC PWM converter represents the ideal means by which input current consumption at variable power factor can be achieved. Thus, the waveform of the current is built according to the frequency of the fundamental wave of the supply network by means of the switching moments that occur at the level of the transistor bridge, determining the quasi-sinusoidal shape, but also possibly the desired phase shift [18]. Since it is a single-phase alternating voltage supply network, the topology of the converter is shown in Fig. 2.1.

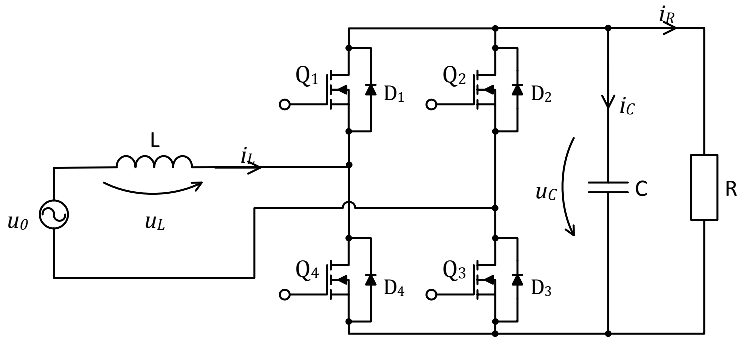

Fig. 2.1 – Single-phase AC/DC PWM converter.

However, the topology of the converter and the way it can be controlled allows its behavior to be changed, becoming a reactive consumer. Thus, the input current can be commanded to be out of phase with respect to the voltage, as exemplified in Fig. 2.6.

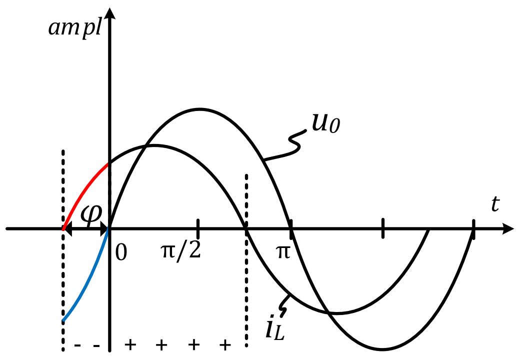

Fig. 2.6–Capacitive phase-shift between input voltage and current: "+" – active power period; "-" reactive power interval;

In this case, a capacitive load behavior is illustrated. The current i_L becomes out of phase before the voltage u_0, considered the phase φ origin, by an angle corresponding to a time duration correlated with the period of the sinusoidal voltage and current signal.

Next, the instantaneous power resulting from such behavior is discussed [19]. It is observed that, during a period, the sign of the power varies, being both positive and negative. The moments of time in which the power shows a certain sign, determine the meaning of the energy transiting the converter. Thus, for a positive value of the instantaneous power, the energy is consumed from the source to the load. For the instant of time when the instantaneous power is negative, the direction of energy transfer reverses, showing a reactive character.

The switching state that captures the negative power moment is shown as state "III" in Fig. 2.7. In this configuration, the voltage u_C is greater than u_0 , which is reverse biased, the difference between u_C and u_0 causing current to flow through transistors Q2 and Q4. However, the direction of the current through the input coil L remains unchanged.

Consequently, the output capacitor, C , discharges more violently, cutting off both i_R and i_L currents.

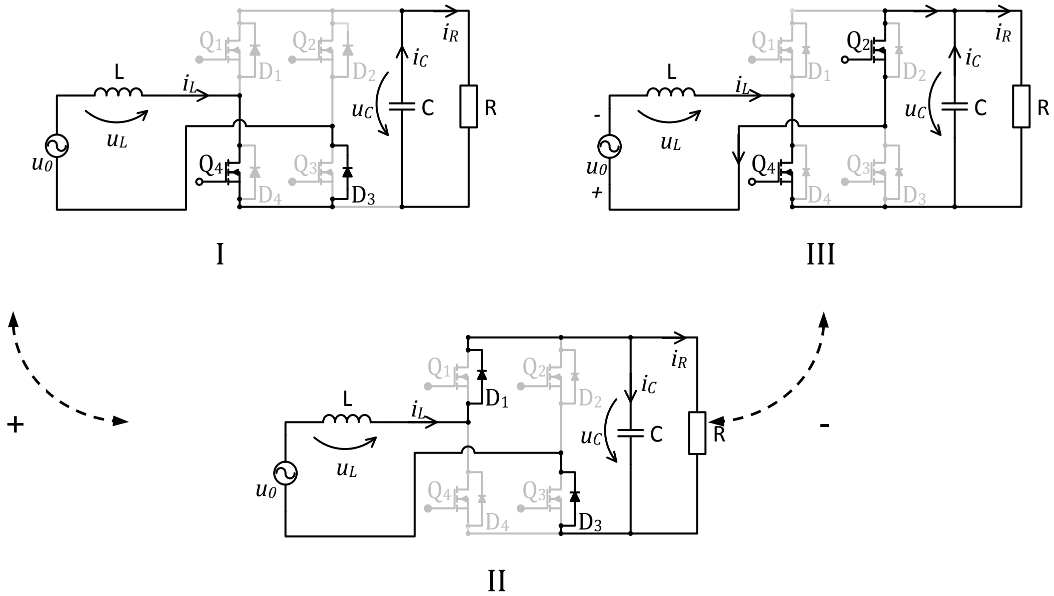

Fig. 2.7 –Switching states for active (I and II) and reactive (II and III) power operation.

The switching states for each direction of power through the circuit are found in Fig. 2.7. Two states can be distinguished for the moments of time when active and reactive power are circulated at the level of the converter. So, considering Fig. 2.6 and Fig. 2.7, it follows that:

– for the duration of a period in which the input voltage and current have the same sign, resulting in active power consumption, the switching states of the converter will be characteristic of hypostases I and II;

– for the duration of time in a period when the input voltage and current are of opposite sign, resulting in an inverse power transit, the switching states of the converter will be characterized by hypostases II and III. In this case, for state II, the sense of the input current remains unchanged, but the input voltage will be considered negative.

It is noted that to ensure the operation of the AC/DC converter correctly, state II is required for each pair of switches to be present. Thus, the aim is to ensure the established value of the voltage at the output of the converter.

To propose a model that would describe the behavior of the converter, regardless of the power factor at which it works, it is desired to observe the variation of the average power with the phase shift. The premise of this analysis is based on the idea that, for a sinusoidal system, the average power characterizes in a unitary way the values of electrical quantities circulated at a given time [19]. Observing how it varies with phase shift could be correlated with the generalized state model and thus yield an overall picture of the converter states, which would also depend on the phase shift angle.

By realizing the expression of the linearized form of the system for the case where the converter operates in reactive mode, it is desired to obtain a general expression for the operation of the converter at a certain given phase shift angle. It was found that the variation of the average power at the input of the converter has a sinusoidal cosine character, with the increase of the phase shift angle. Thus, for a zero-phase shift, the average value of the input power has a maximum value, and for a phase shift of $\pi/2$ is zero.

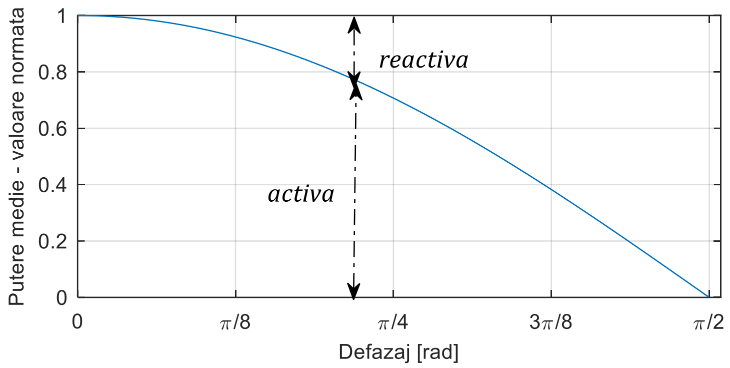

Fig. 2.10 – Active and reactive weighing of the maximum power, with phase-shift variation.

In Fig. 2.10 it is presented the distribution mode, as a share of the total average power of the average active and reactive power, at a certain given phase shift. It is observed that, with the decrease in the value of the active power, the reactive power will increase and vice versa. The representation of this dependence can be realized as an expression of some coefficients correlated with the two values of active and reactive power:

$$q_1 = \cos(\varphi)$$
$$q_2 = 1 - \cos(\varphi)$$

where q_1 is the coefficient corresponding to the average value of the active power, q_2 is the coefficient corresponding to the average value of the reactive power, and φ is the phase shift angle, so that:

$$q_1 + q_2 = 1$$

Transfer functions correlated with the phase shift were determined by operating with symbolic elements in the MATLAB calculation program. Thus, the transfer functions that correlate the output quantities with the input voltage are the following:

$$\frac{\tilde{I}_L(s)}{\tilde{U}_0(s)} = \frac{(RCs + 1 - 2Dq_2)(q_1 - q_2)}{RCLs^2 + Ls(1 - 2Dq_2) + R[(D^2(1 - q_2^2) - 2D + 1]}$$

$$\frac{\tilde{U}_C(s)}{\tilde{U}_0(s)} = \frac{R(q_1 - q_2)[1 - D(1 + q_2)]}{RCLs^2 + Ls(1 - 2Dq_2) + R[(D^2(1 - q_2^2) - 2D + 1]}$$

For small variations of the filling factor, the dependence of the output quantities is represented by the expressions:

$$\frac{\tilde{I}_L(s)}{\tilde{D}(s)} = \frac{(RCs + 1 - 2Dq_2)(D - 1) - (1 - Dq_1)}{RCLs^2 + Ls(1 - 2Dq_2) + R[(D^2(1 - q_2^2) - 2D + 1]} \cdot \frac{-q_1 U_0}{(D - 1)^2}$$

$$\frac{\tilde{U}_C(s)}{\tilde{D}(s)} = \frac{Ls + R[1 - D(q_1 - 2q_2)](D - 1)}{RCLs^2 + Ls(1 - 2Dq_2) + R[(D^2(1 - q_2^2) - 2D + 1]} \cdot \frac{-q_1 U_0}{(D - 1)^2}$$

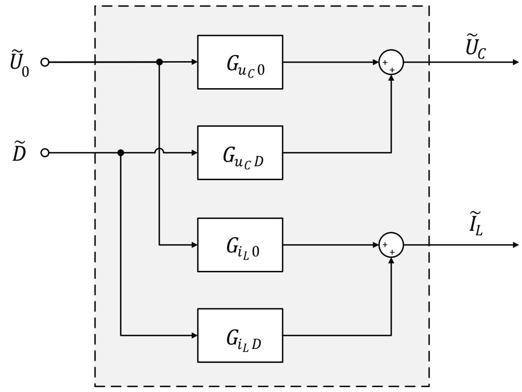

Fig. 2.11 –General block diagram of the converter.

3 UNITY POWER FACTOR OPERATION. SIMPLE LINE CONDITIONING OF THE AC GRID

In this chapter, the establishment of the constraints facing the operation of the converter was necessary to determine the parameters and passive elements at its level. Since the converter operates at unity power factor, achieving simple conditioning of the supply network, the problem of its input current aspect arose. Following the norms in force at European and international level and correlating aspects such as: maximum and minimum power level, switching frequency, harmonic distortion factor - THD, the value of the input inductance of the converter was determined. A first remark in this regard could be made vis-à-vis the minimum power level at which the quality parameters of the electricity absorbed from the network are maintained. It can therefore be concluded that a lower limitation of the power value appears for operation at a reduced THD factor. However, a compromise based on operating the converter for short periods of time at low power levels, led to the acceptance of a THD factor of about 20% for the input current, this being reduced to 8% in the case of operation at power nominal, which is a positive aspect.

As for the output voltage filtering stage, the references related to its maximum ripple led to the dimensioning of the capacitance value of the characteristic capacitor of this stage. References dealing with aspects related to direct current micro-grids, as well as amplitude and ripple values circulated at their level, were tracked.

In order to realize the control structure, for simple conditioning operation, the average input current control model was considered, which determined the control scheme used. Knowing the values of the circuit elements, the system behavior of the converter was studied, after which the specific values of the compensator for the current loop and the regulator for the voltage loop were determined. Regarding the constraints in carrying out this approach, the ways in which the input current and the output voltage would vary over time were considered, trying to correlate them with the physical aspects and limitations that would be encountered in operation. Based on the analysis, the desired converter response parameters were achieved.

In the last part of this chapter, the author wanted to observe the behavior of the converter seen as a system when the operation is carried out at the minimum power level. Here it was possible to see how the variation of the output voltage and the current at the input of the converter no longer respected the previously specified parameters. This is because the voltage loop regulator is sized to operate at rated power. However, the stabilized mode of operation is reached, and the operation is not affected, apart from the non-observance of the parameters of the transient mode. Related to this aspect, a possible solution would be a non-linear control by dynamically adjusting the regulator parameters in the system, which would correspond to the load level of the converter. In this way, both a transient and a steady-state response satisfying the operating parameters could be obtained. Thus, the implementation of the nonlinear control method with gain scheduling of the regulator coefficients for the converter control loop was approached. Based on predetermined values, which guaranteed operation within the limits of the imposed parameters, specific values of intermediate power points were determined, by means of their interpolation. Finally, the behavior of the converter was observed through simulation, in the case of applying the non-linear control method, the variation mode of the output voltage presenting a better performance in this case.

The operation of the unitary power factor converter would, according to the aspects mentioned in the first part of the thesis, be equivalent to the attribute of simple line conditioning of the alternating current supply network. Thus, at the common coupling point (PCC), the behavior of the converter would emulate a resistive consumer, therefore not contributing to the loading of the network with reactive energy. In order to be able to observe how this aspect is achievable, the passive elements of the converter will be determined, and then a control scheme suitable for this mode of operation of the ac/dc converter will be proposed and realized.

Since the mode of operation of the converter followed by the control scheme is to achieve unity power factor operation, in addition to the DC output voltage, a controlled quantity will also be the input current to the converter. In this sense, a control method will be applied through the value of the average input current, according to [18]. Through this control method, the diagram shown in Fig. 2.11 from the previous chapter can be represented as in Fig. 3.2.

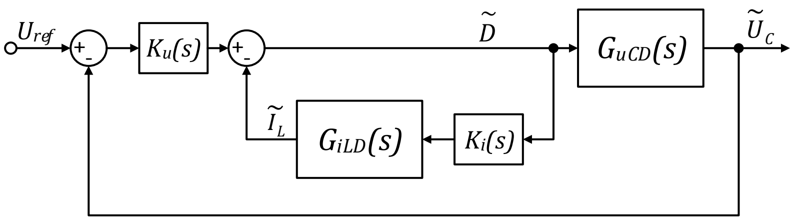

Fig. 3.2 - Average current mode control block diagram.

It is mentioned that the inner current loop of the studied system model is required to be faster than the one that regulates the voltage. In this sense, there will be no significant intervention in regulating this aspect [18]. According to the recommendations [18] and considering the fact that the chosen switching frequency is 100 kHz, in order to mitigate the presence of switching noises and to filter possible high-frequency disturbances, it is desired to reduce the cut-off frequency to a lower value. In order to obtain the desired cut-off frequency, but at the same time not to change the amplification factor of the system at low-frequency, one opts for modeling the compensator, with a phase deficit (lag-compensator) [20].

$$K_i(s) = \frac{\omega_p}{\omega_z} \cdot \frac{s + \omega_z}{s + \omega_p}$$

In Fig. 3.19, in the time interval marked with A, the form of the modulation signal is represented at the time of application of the compensator, and in the interval marked with B, the same signal, without compensation. It can be easily seen that the noise level is significantly reduced following the current loop compensation, thus determining a more faithful sinusoidal reference for the SPWM control signal generation stage.

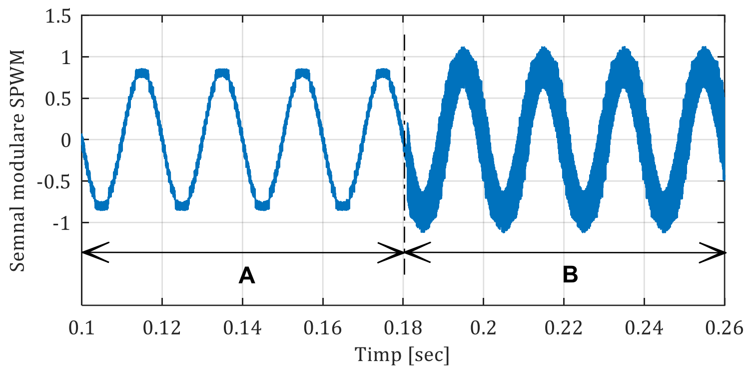

Fig. 3.19 –Effect of current loop compensation: A – with compensation; B – without compensation.

Changing the power level, respectively the load of the converter, determines a behavior that does not guarantee the performance conditions imposed for any operating point. This is due to the fact that the parameters of the $K_u(s)$ regulator have been preset, on the simplified model, for a certain set of values characteristics of operation at nominal power. Thus, in the case of changing the converter load, it no longer presents a linear system character, but one in which the parameters can vary linearly (Linear Parameter Varying - LPV) [21], having different operating points for each set of parameter configurations. In this sense, it is possible to modify the regulator values by monitoring the operating conditions from a given moment using the gain scheduling method [22].

Based on the system model, it was used to determine the values of the coefficients k_P and k_I from the relationship, related to the regulator, for different values of the power level. For this, the "PID Tuner" interface from the Control System Toolbox of MATLAB was used. The response of the system in Fig. 3.2, when applying a unit-step input to each configuration, is represented below:

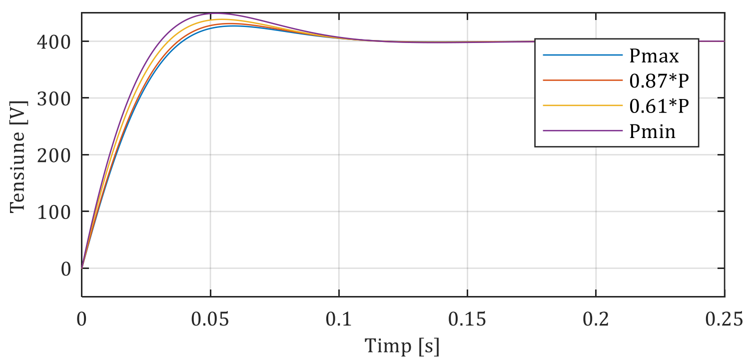

Fig. 3.22 –Output voltage response, at different power output power levels.

Here it is observed how, regardless of the power level, the system responses fall within the stated performance requirements.

Considering the fact that the system is interpreted as one whose parameters (power) vary, and the linear model and implicitly the regulation coefficients have been determined at specific operating points, it is aimed to discretize their values for intermediate points. This will increase the number of possible operating configurations without them being individually determined as before. The gain scheduling control method under discussion relies on this technique to provide system performance and accuracy. Thus, based on the preset values, using MATLAB - PID Tuner, a series of new values, intermediate to those mentioned, are interpolated for the coefficients and of the $K_u(s)$ regulator.

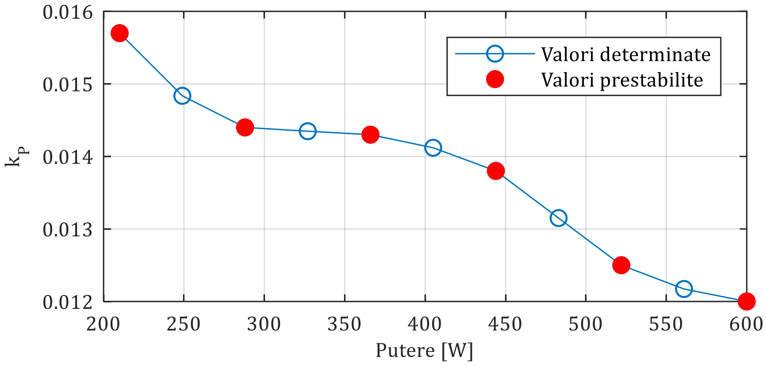

a)

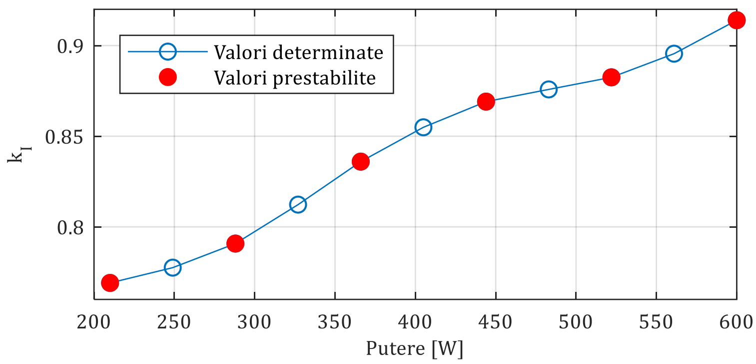

b)

Fig. 3.26 – Predetermined and interpolated values of: a) k_P coefficient; b) k_I coefficient

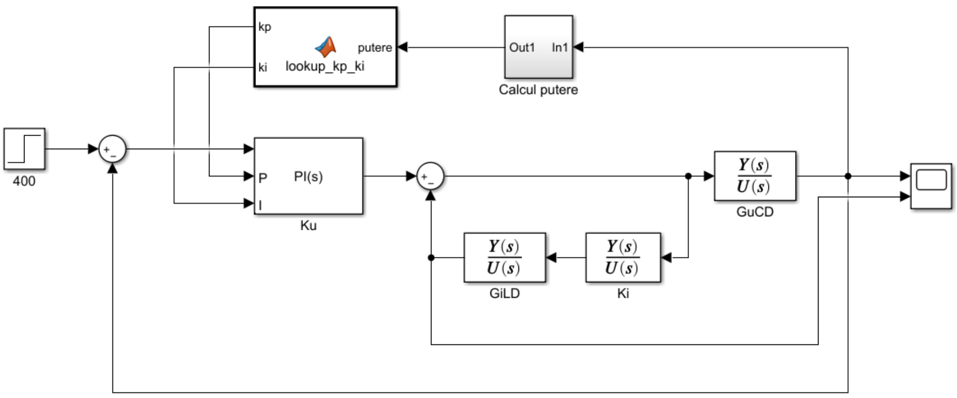

Fig. 3.28 - Simulink model of the system, with the nonlinear control implemented.

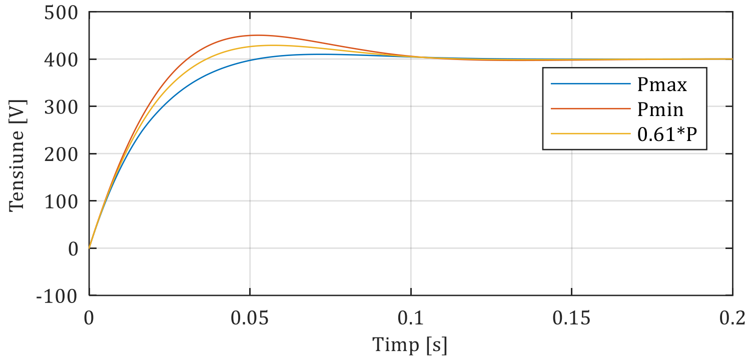

a)

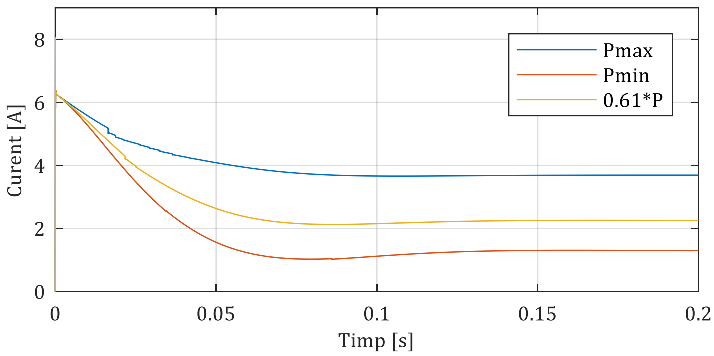

b)

Fig. 3.29 - System response using the nonlinear control method: a) output voltage; b) input current.

4 ACTIVE POWER FACTOR COMPENSATION AS A SECONDARY ELECTRONIC FUNCTION

The aspect that is wanted to be discussed in this chapter refers to the possibility of obtaining the modification of the behavior of the AC/DC. converter so as to actively participate in improving the quality of electricity at the PCC of the supply network. In this sense, the assignment of a secondary electronic function for certain operating conditions would exclude the need to introduce new equipment into the system, which would be dedicated to achieving reactive energy compensation at the PCC. Therefore, it can be stated that, without the need for additional physical equipment, the power density of the system has been increased, not by increasing the installed power, but by reducing the "equivalent volume".

A possible way of exposing an AC supply network is shown in Fig. 4.2. In this representation, the alternating U_{PCC} voltage source provides the power and implicitly the i_{PCC} current required by the consumers found at the common coupling point (PCC) [16]. To simplify the diagram, only two consumers have been represented, namely: a linear consumer that can exhibit an inductive character and a consumer that represents the AC/DC PWM converter studied, the latter charging the power from its output to a resistive load. The currents i_L and i_{RL} , absorbed by the consumers connected to the PCC, will compose the current charged by the supply network.

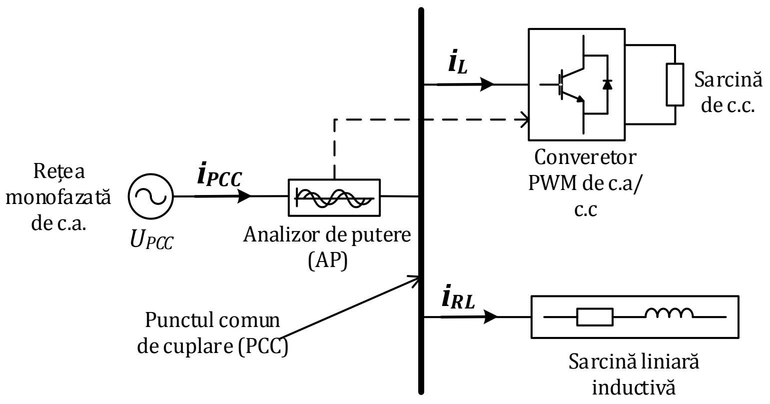

Fig. 4.2– Simplified diagram of an AC supply grid.

The required I_Q reactive current level is directly correlated with the phase shift angle, φ , and can be determined by means of a power analyzer (AP) located before the PCC, as can be seen in Fig. 4.2. Knowing this value and having the possibility to control the I_L current absorbed by the converter, one can resort to the orientation of the converter I_L^* current phasor, considering I_Q. Thanks to this aspect, the power network will no longer have to discharge reactive energy into the PCC. The I_Q reactive current circulation will take place between the inductive consumer and the AC/DC converter.

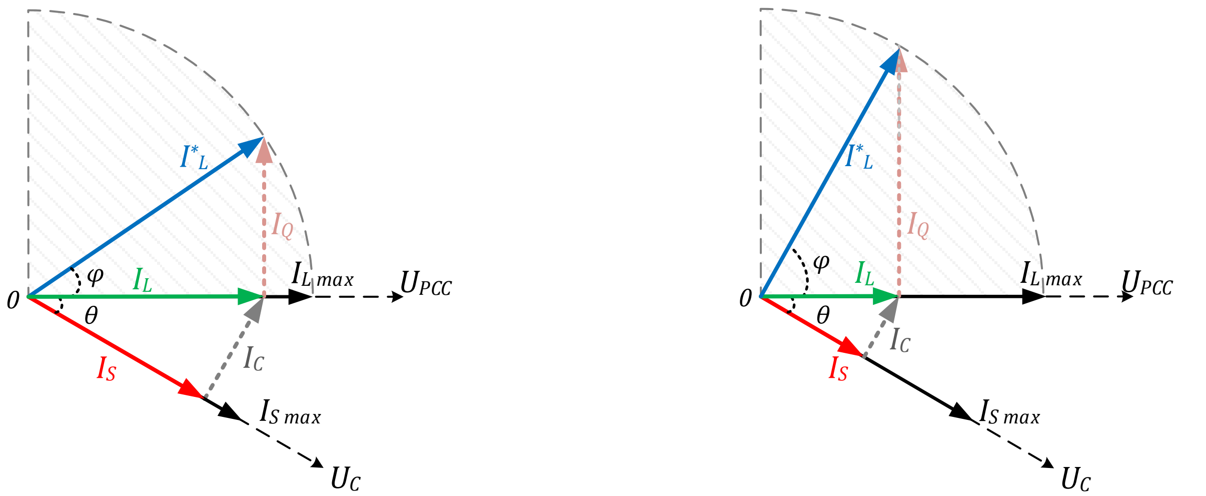

a) high output power b) low output power

Fig. 4.6 – Phasor diagram of the active power compensation at PCC.

In Fig. 4.6 the phasor diagrams for the operation of the converter at a high-power level and at a lower power level are shown comparatively. This can be seen by following the amplitude of the phasor describing the output current, which is smaller in the case of representation "b)". Thus, assuming that a reactive, inductive, I_Q current appears at the PCC, in order to achieve its compensation, it is necessary to phase-shift the input current of the converter, with a capacitive angle φ, which will lead to the formation of the phasor I_L^*. The maximum amplitude of the resulting phasor will be limited by the $I_{L\,max}$ value, and according to the geometric representation, it will describe an arc of a circle. I_L^* projection on the U_{PCC} reference will represent the absorbed active current, necessary to maintain the voltage and power level at the output of the converter, being correlated with the value of the I_S load current.

Regarding the converter control technique, the proposed approach will be similar to the previous one. The "classic" scheme will be implemented with an inner loop for the input current and an outer one that will control the output voltage. Considering the phasor diagrams in Fig. 4.6, it is proposed to modify this "classic" scheme, as exemplified in Fig. 4.10.

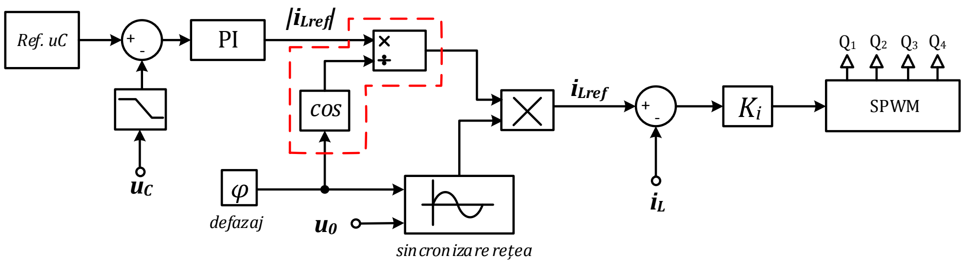

Fig. 4.10 – Proposed enhancement of the control loop.

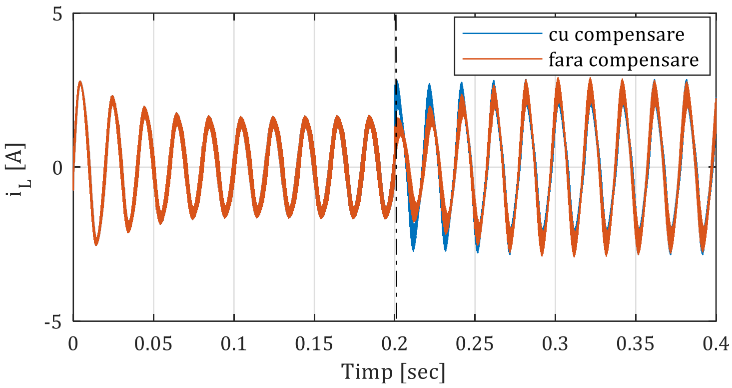

Fig. 4.11 –Input converter current behavior.

As can be seen in Fig. 4.11, the response of the input current, when the control loop compensation is applied, becomes faster, compared to the "classical" system. It is pre-amplified to the reference value, thus reducing the effort of the PI controller in the feedback loop and increasing the speed of response.

The output voltage, measured after the simulation, is shown in Fig. 4.12. Probably in this case, the effect of feedback loop compensation is best represented. It can be seen how, unlike the initial response, which shows a transient regime where the average value of the voltage decreases with respect to the reference, in the case of the compensation control system, the response is much firmer.

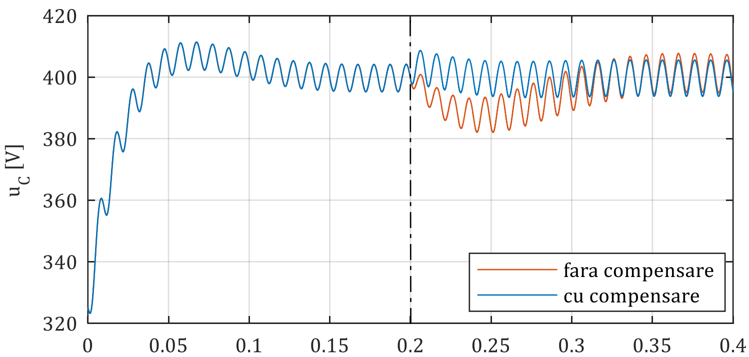

Fig. 4.12 – Converter's output voltage behavior.

The nonlinear control method, through gain scheduling [23], [24], previously applied to the operation of the converter for power values lower than the nominal one, is proposed to be adapted and applied in the present case as well. In the present situation, in addition to the possible variation of the power at the output of the converter, there is also the criterion of the variation of the phase shift angle. Thus, if in the previous case, only one variable was considered, namely the power, this time the value of the phase shift will also have to be considered. Fig. 4.14 show the values obtained in terms of the amplification k_p factor. The values of the gain coefficients for the PI controller will be characterized by the generic function $k = f(P, \varphi)$.

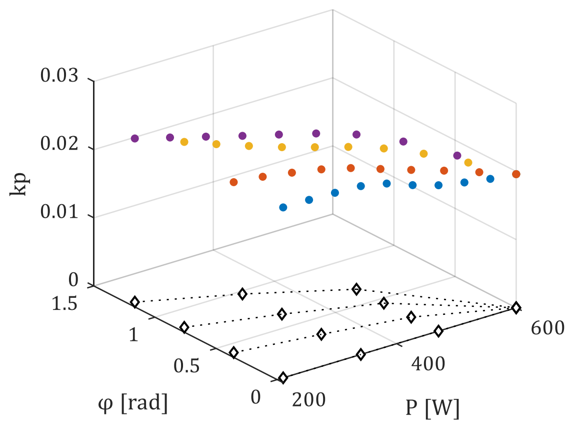

Fig. 4.14 – Representation of k_p interpolated values.

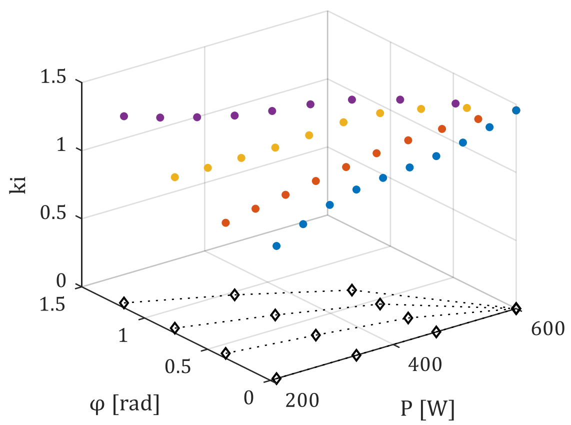

Fig. 4.16 – Representation of k_i interpolated values.

In order to test the behavior of the implemented control strategy, the simulation of the operation of the converter at different power levels and phase shift of the input current was carried out. In Fig. 4.20 the control structure of the studied converter can be seen. Unlike the previous configuration, the elements proposed in this chapter can be observed, namely: feedback loop compensation and the algorithm for determining the amplification factors for the PI regulator, as a component part of the structure.

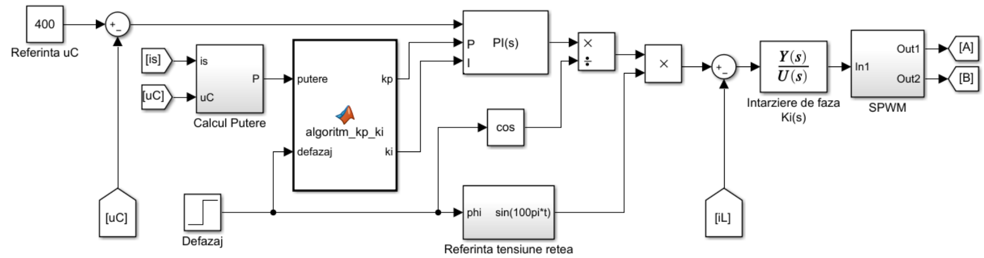

Fig. 4.20 - Converter's control scheme for applying reactive power compensation at PCC.

The implementation of the circuit was realized by means of the PLECS Blockset modeling support, together with the emulation of the common coupling point, in the framework of Matlab-Simulink. This stage is represented in Fig. 4.21.

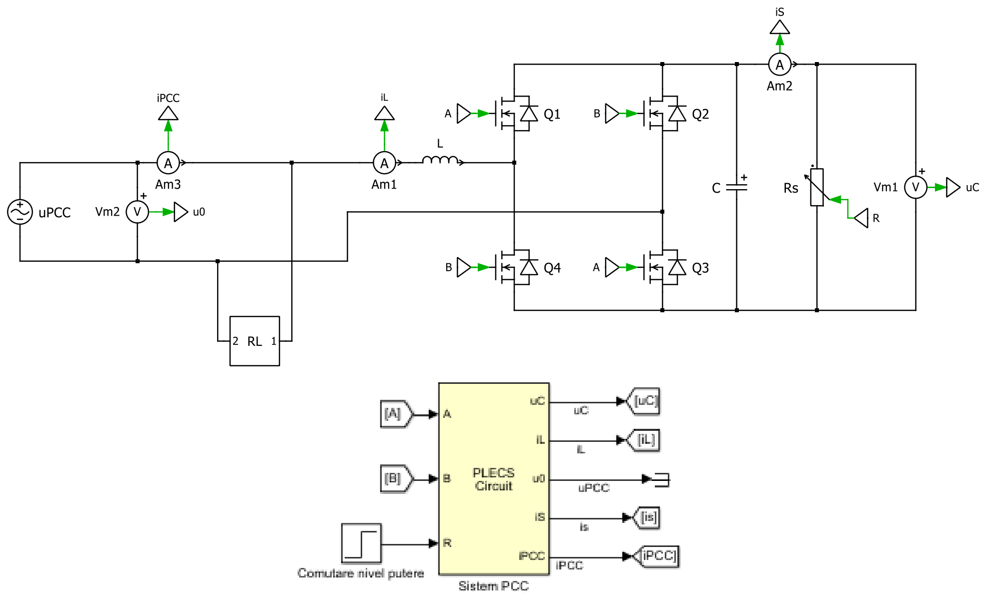

Fig. 4.21 –The converter and PCC models, and their PLECS Blockset representation.

In Fig. 4.22, the obtained results can be observed. The simulation runs as follows: initially, the converter operates at unity power factor, at the preset power level. At the time of 0.15 seconds, the value of the phase shift angle for the input current is changed by a step signal, from the value of zero, to the maximum allowed for the respective power level.

In each scenario presented, it is observed how, when active compensation is applied by the converter, the current is brought into phase with the voltage reference, at a power factor around unity. The most obvious aspect regarding the compensation of the reactive component of the current is the fact that the amplitude of the current becomes smaller. This is achieved without changing the structure of the supply network by removing or adding consumers. The secondary electronic function of the converter and the way it changes its behavior at the input provides a new source of reactive energy, which can take the place of the mains supply.

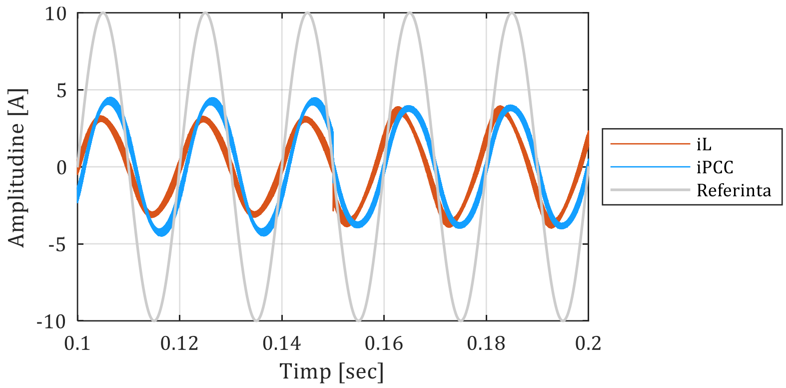

a) 78% of maximum power

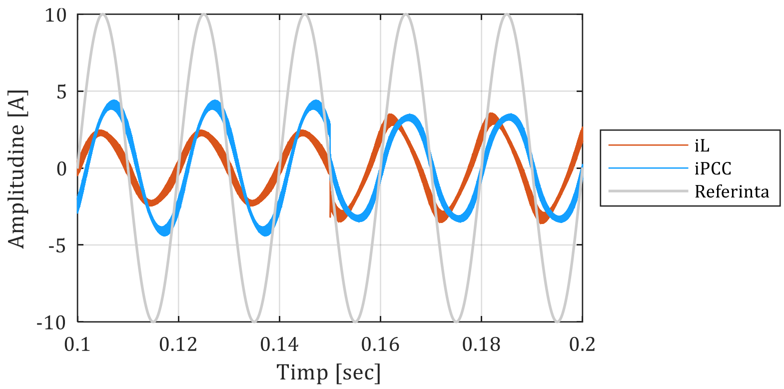

b) 57% of maximum power

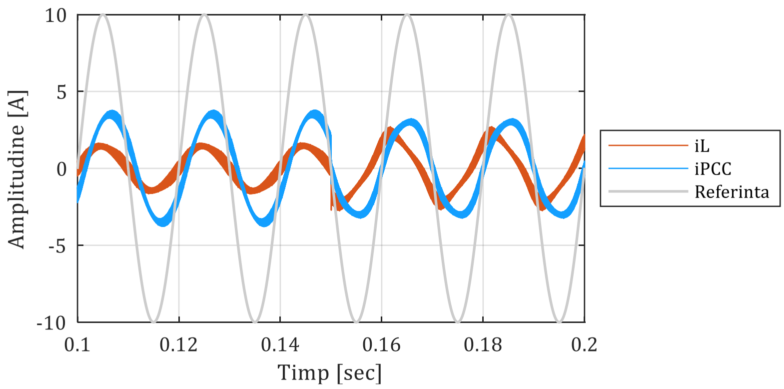

c) 35% of maximum power

Fig. 4.22 –Reactive power compensation scenarios, for the converter operating at various power levels.

5 THE IMPLEMENTATION AND VALIDATION OF THE PROPOSED CONTROL STRATEGY

The current chapter traces the process of implementing the algorithm and control strategy for the AC/DC converter through a hardware-in-the-loop (HiL) simulation. This stage is related to the numerical simulation, previously carried out with calculation programs. Thus, by using an interface that emulates the behavior of devices and electronic equipment found at the level of the studied system, it is desired to verify and validate the control strategy, under the conditions of its implementation at the level of a dedicated device, such as a digital signal processor (DSP).

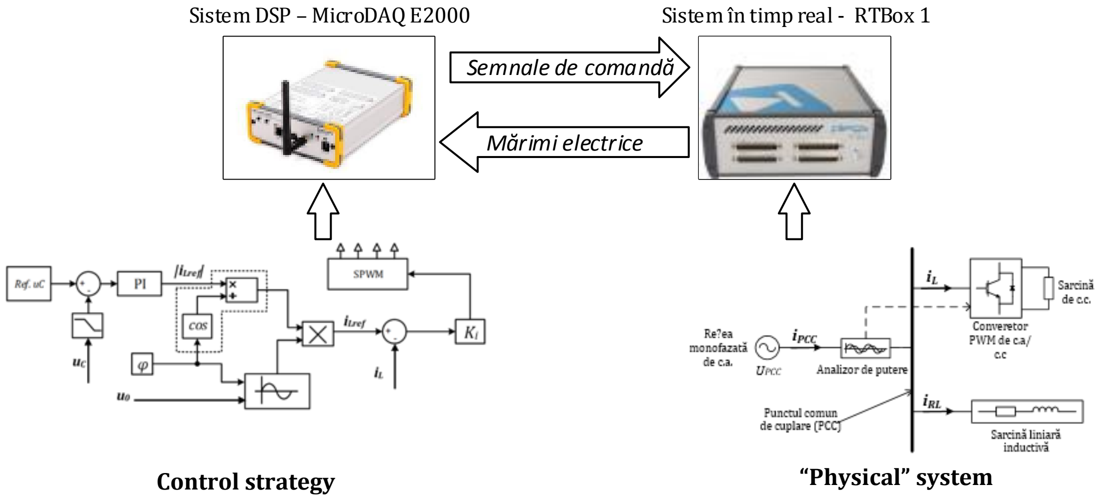

Fig. 5.1- HiL implementation diagram.

In Fig. 5.1 is the schematic diagram of the HiL type implementation. In this sense, the performance of the control strategy that uses the monitoring and regulation of "physically-equivalent" quantities, reproduced by the real-time simulation device (HiL), PLECS RT Box 1 [25], is followed. The latter will emulate the behavior of the entire physical system: the power grid, the connected consumers of the PCC, the AC/DC PWM converter, etc. and will react as such upon receiving command signals from the control equipment, represented by the DSP processor-based system, MicroDAQ E2000 [26].

In the previous chapter, recourse was made to the application of the nonlinear control method to the variation of both the power and the phase shift, justifying the secondary electronic function of the PWM rectifier to achieve the active compensation of the reactive energy circulation at the PCC. However, the system was studied in isolated conditions, not being able to decide on its own when and to what extent it is able to provide support in reactive power level management. Next, the author proposes the implementation of a method that allows the converter to provide support, optimally, for the compensation of reactive currents from the PCC. In this sense, a series of observations and constraints are provided, which need to be justified in advance:

– the operation of the converter, normally, will be allowed at a power factor $\cos(\varphi) \geq 0{,}988$, which corresponds to a radian phase shift angle $\varphi \leq 0{,}15$;

– the primary function of the converter will be to ensure at the output a continuous, stabilized voltage of a predefined value;

– the converter will not operate outside the minimum and maximum power limits for which it was designed;

– the algorithm must permanently ensure the value of the phase shift angle of the reference signal, for the input current from the converter.

The quantities found in the algorithm diagram in Fig. 5.6 represent quantities measured at the level of the AC/DC PWM converter, preset quantities, or determined algebraically, as follows:

Default

P – nominal power;
U – supply voltage;
uC – output voltage;
Ismax – maximum amplitude of the output current;

ILmax – the maximum amplitude of the input current.

Measured

iS – output current;
IPCC – current amplitude at PCC;
– the phase shift at PCC.

Determined

IL – the real component of the input current;
IQPCC – the amplitude of the reactive component of the current at PCC;
IQmax – the maximum available compensation value of the PWM rectifier;
φ_{max} – the maximum allowed phase shift angle of the input current in the AC/DC PWM converter;
φ_{set} – the reference value for the phase shift of the input current in the AC/DC PWM converter.

Initialization

φ_0 – initialization variable of the phase shift;
Δ - amount of increase.

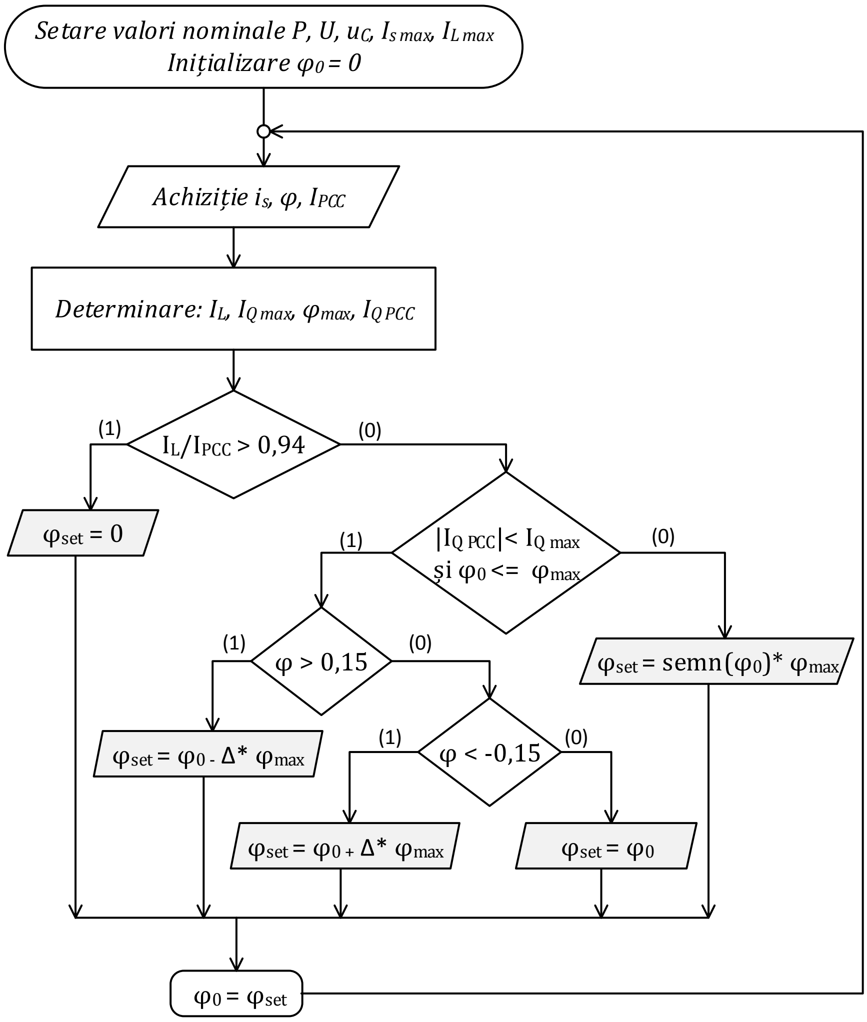

Fig. 5.6 –Algorithm flow diagram.

In Fig. 5.9 is a diagram showing how the signals of the electrical quantities are routed and monitored in the real-time simulation.

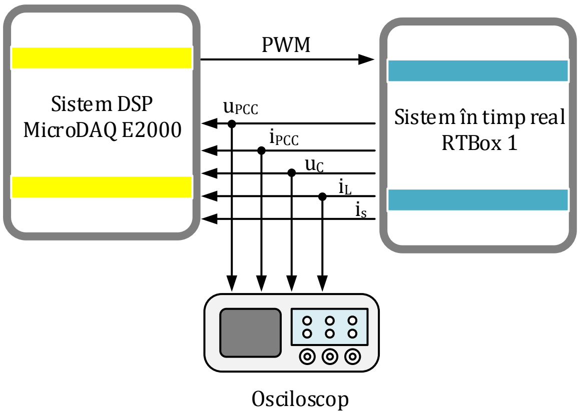

Fig. 5.9 – Exchanged signals between the HiL devices.

The real-time simulation stand is represented in Fig. 5.10. During execution, the measured electrical quantities are acquired by the DSP system and then used within the control scheme. The response, in the form of the PWM control signal, is fed back to the system in real time, and implicitly to the switching network at the AC/DC PWM converter level emulated.

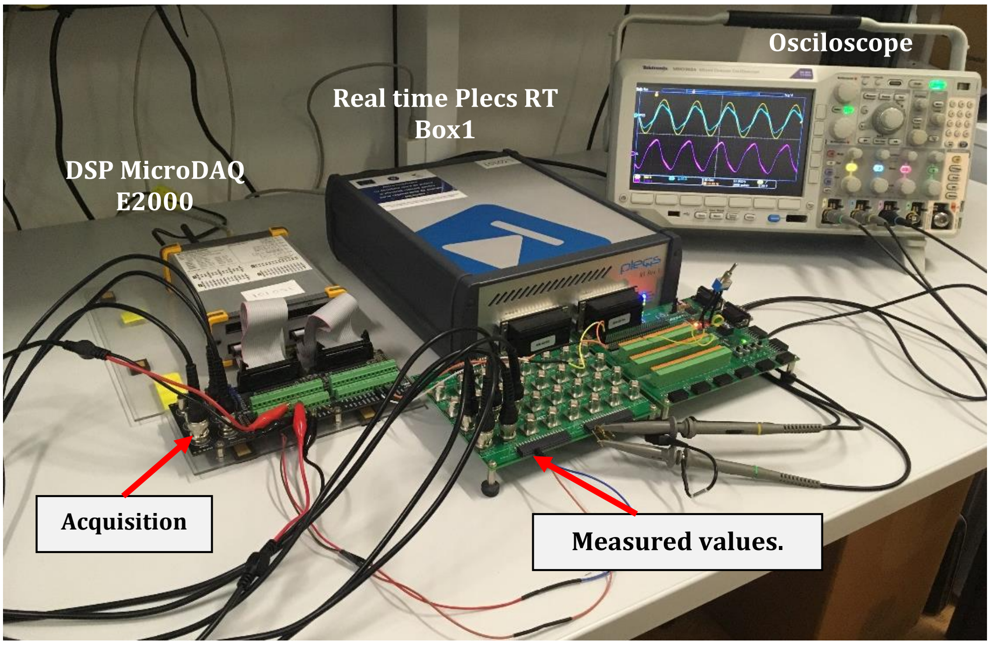

Fig. 5.10 – The Hardware-in-the-loop setup

A series of situations have been studied, including different load levels for the converter, but also the presence or absence of inductive consumers at the common coupling point of the network.

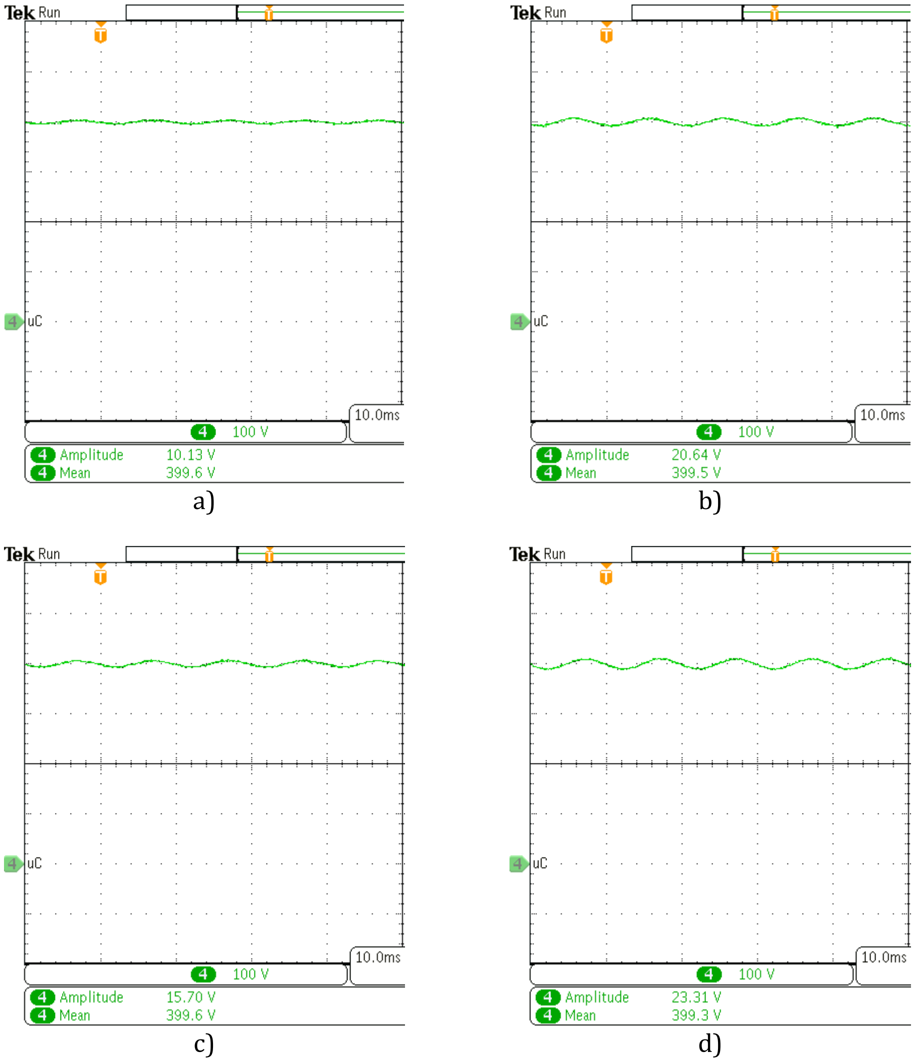

Fig. 5.11- Output voltage of the converter at : a) minimum power; b)minimum power and reactive compensation; c)56% loading and reactive compensation; d) maximum power.

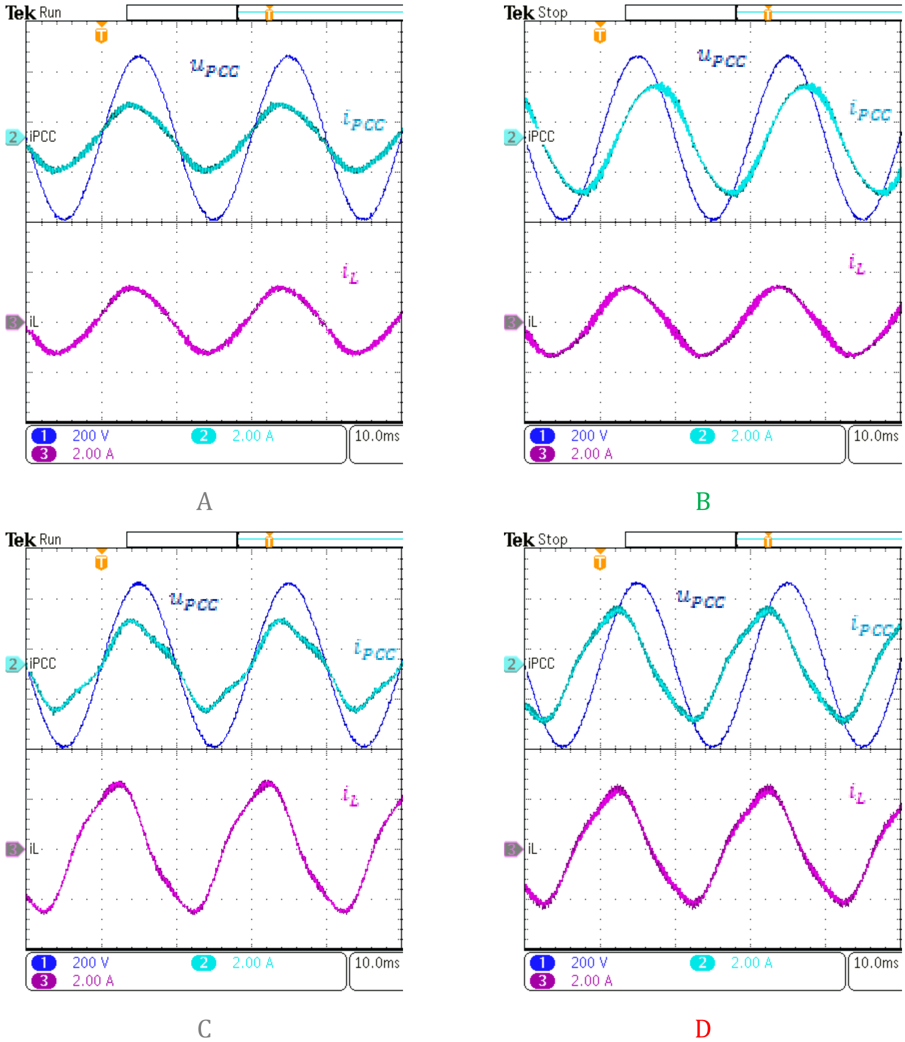

Fig. 5.12 - The behavior of the converter's input current and the PCC current, when connecting and disconnecting an inductive load at PCC: A – without inductive load; B – connecting the load; C – reactive power compensation by the converter; D – disconnecting the inductive load.

To outline a more general picture, the magnitudes of the current and the phase shift angle were used to determine the value of the apparent power, charged by the supply network to the PCC. In this situation, a number of cases have been observed in which reactive energy compensation is achieved. Their configuration is outlined in Table 5.2. Thus, for two cases, the converter was at minimum load, and for the other two, at approximately half of the nominal power.

Tabelul 5.2- Different configurations for observing the power behavior at PCC.

Case	***Converter Loading***	***Power consumers at PCC***	
		Consumer 1	***Consumer 2***
a	*30% - minimum loading*	*X*	
b		*X*	*X*
c	*56% loading*	*X*	
d		*X*	*X*

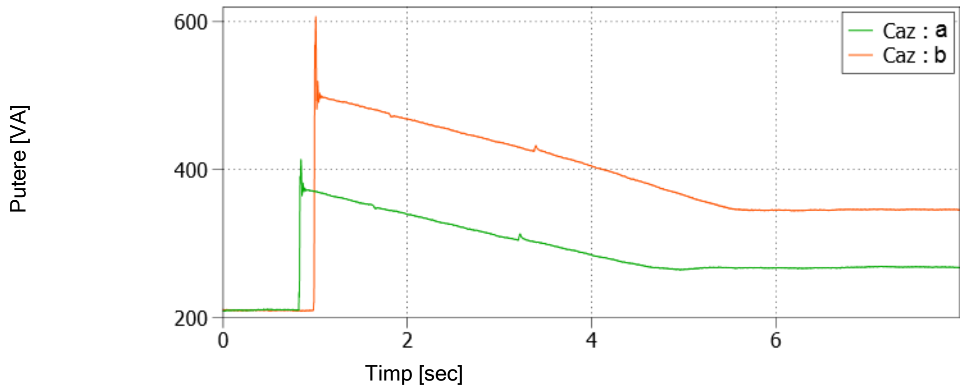

a) minimum loading of the AC/DC converter.

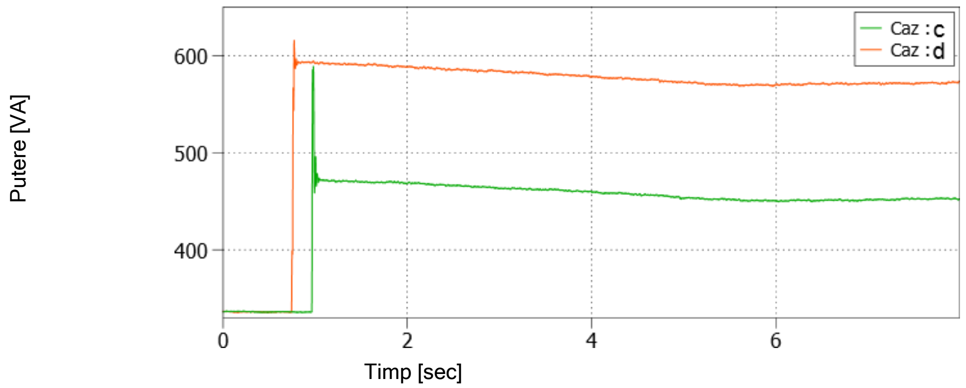

b) 56% loading of the AC/DC converter.

Fig. 5.14 - Apparent power variation at the PCC.

6 FINAL CONCLUSIONS AND CONTRIBUTIONS

The original aspects found in the present work are reflected in the development, analysis and testing of a control method, which not only facilitates the smooth operation of an AC/DC PWM single-phase converter but allows the integration of a secondary electronic function at its level. This was possible by developing a decision-making algorithm and optimizing the control strategy, so as to allow the use of the power reserve of the converter, in order to increase the quality of the electrical energy at the common point of coupling to the AC supply network. Another aspect with a note of originality, refers to the expansion of the concept of increasing the power density, at the system level. Thus, for the realization of this additional function, a reserve of the already installed power is used, and the introduction of additional equipment is no longer necessary.

The contributions of the author of this thesis are listed as:

Chapter 1 - Study regarding the current state regarding the topologies of single-phase AC/DC PWM converters and their characteristic control strategies;

The study of the methods of achieving synchronization through phase-locking loops. C

Conducting a synthesis and comparison of the main synchronization techniques based on phase locked loops;

Introducing the problem of power density at the level of a system;

A number of the aspects treated in this chapter are based on two published works.

Chapter 2 - Analysis and mathematical description of the operation of the converter in active and reactive power mode;

Development of a mathematical model characteristic of operation in reactive mode;

Integration of the developed mathematical model into the general operating model of the converter;

A number of the results obtained in this chapter were presented through a paper.

Chapter 3 - Sizing the converter and implementing a control strategy for the operation of the converter at unity power factor;

Implementation of a non-linear control method, based on operating points with known performance;

Simulation and analysis of control system behavior.

Chapter 4 - Optimization of the control loop based on the results obtained from the interpretation of the characteristic phasor diagrams of the converter;

Implementation of a management and optimization algorithm for non-linear control, in case of variation of two parameters (output power and phase shift);

Proposal and dimensioning of a synchronization stage, based on a phase-locking loop;

MATLAB Simulink – PLECS Blockset co-simulation analysis of control loop and converter;

A number of the results obtained in this chapter were presented through two papers.

Chapter 5 - The transposition of the control loop elements in the discrete domain, in order to be implemented on hardware support;

Development and proposal of a decision-making algorithm, in order to manage the behavior of the converter vis-à-vis the power network;

Analysis of the control method developed by means of a "Hardware-in-the-Loop" real-time simulation;

Interpretation and validation of the results obtained from the HiL analysis.

A number of the results found in this chapter have been submitted for a patent application.

References

[1] S. Parhizi, H. Lotfi, A. Khodaei, and S. Bahramirad, "State of the Art in Research on Microgrids: A Review," *IEEE Access*, vol. 3, pp. 890–925, 2015, doi: 10.1109/ACCESS.2015.2443119.

[2] N. W. A. Lidula and A. D. Rajapakse, "Microgrids research: A review of experimental microgrids and test systems," *Renewable and Sustainable Energy Reviews*, vol. 15, no. 1, pp. 186–202, Jan. 2011, doi: 10.1016/j.rser.2010.09.041.

[3] V. M. Suciu, L. N. Pintilie, **S. I. Salcu**, P. D. Teodosescu, T. Pana, and Z. Mathe, "Analysis of an Independent Double Boost Interleaved Converter in a Renewable Energy Application," in *Proceedings of Seventh International Congress on Information and Communication Technology*, Singapore, 2023, pp. 539–548. doi: 10.1007/978-981-19-2394-4_49.

[4] V. M. Suciu, **S. I. Salcu**, A. M. Pacuraru, L. N. Pintilie, N. C. Szekely, and P. D. Teodosescu, "Independent Double-Boost Interleaved Converter with Three-Level Output," *Applied Sciences*, vol. 11, no. 13, Art. no. 13, Jan. 2021, doi: 10.3390/app11135993.

[5] J. J. Justo, F. Mwasilu, J. Lee, and J.-W. Jung, "AC-microgrids versus DC-microgrids with distributed energy resources: A review," *Renewable and Sustainable Energy Reviews*, vol. 24, pp. 387–405, Aug. 2013, doi: 10.1016/j.rser.2013.03.067.

[6] D. Fregosi *et al.*, "A comparative study of DC and AC microgrids in commercial buildings across different climates and operating profiles," in *2015 IEEE First International Conference on DC Microgrids (ICDCM)*, Atlanta, GA, USA, Jun. 2015, pp. 159–164. doi: 10.1109/ICDCM.2015.7152031.

[7] I. Nutkani, P. Loh, and F. Blaabjerg, "Power flow control of intertied ac microgrids," *Power Electronics, IET*, vol. 6, pp. 1329–1338, Aug. 2013, doi: 10.1049/iet-pel.2012.0640.

[8] I. U. Nutkani, P. C. Loh, P. Wang, T. K. Jet, and F. Blaabjerg, "Intertied ac–ac microgrids with autonomous power import and export," *International Journal of Electrical Power & Energy Systems*, vol. 65, pp. 385–393, Feb. 2015, doi: 10.1016/j.ijepes.2014.10.040.

[9] G. C. Kryonidis, E. O. Kontis, A. I. Chrysochos, K. O. Oureilidis, C. S. Demoulias, and G. K. Papagiannis, "Power Flow of Islanded AC Microgrids: Revisited," *IEEE Trans. Smart Grid*, vol. 9, no. 4, pp. 3903–3905, Jul. 2018, doi: 10.1109/TSG.2018.2799480.

[10] G. Agundis-Tinajero, J. Segundo-Ramírez, N. Visairo-Cruz, M. Savaghebi, J. M. Guerrero, and E. Barocio, "Power flow modeling of islanded AC microgrids with hierarchical control," *International Journal of Electrical Power & Energy Systems*, vol. 105, pp. 28–36, Feb. 2019, doi: 10.1016/j.ijepes.2018.08.002.

[11] X. Zhou, K. Wei, Y. Ma, and Z. Gao, "A Review of Reactive Power Compensation Devices," in *2018 IEEE International Conference on Mechatronics and Automation (ICMA)*, Aug. 2018, pp. 2020–2024. doi: 10.1109/ICMA.2018.8484519.

[12] C. Wessels, S. Grunau, and F. Fuchs, "Current Injection Targets for a StatCom under Unbalanced Grid Voltage Condition and the Impact on the PCC Voltage," Jan. 2011.

[13] O. K. Shinde and V. R. S. V. B. Pulavarthi, "STATCOM converters and control: A review," in *2017 International Conference on Data Management, Analytics and Innovation (ICDMAI)*, Feb. 2017, pp. 145–151. doi: 10.1109/ICDMAI.2017.8073500.

[14] G. Shahgholian and J. Faiz, "Static Synchronous Compensator for Improving Performance of Power System: a Review," vol. 5, no. 5, p. 11, 2010.

[15] R. Marschalko, C. Salomir, and M. Bojan, "Line Conditioning with the help of the PWM DC Converters – An Alternative to the Power Conditioning Converters," *Acta Electrotehnica*, vol. 46, no. 3, pp. 141-148, 2005.

[16] R. Paku, C. Popa, M. Bojan, and R. Marschalko, "Appropriate Control Methods for PWM ac-to-dc Converters Applied in Active Line-Conditioning," in *2006 12th International Power Electronics and Motion Control Conference*, Aug.2006, pp.573-579.

[17] M. Bojan, "Strategii de Comandă și Reglare Adecvate Conversiei de C.A/C.C. cu Condiționarea Rețelei de Curent Alternativ," Universitatea Tehnică din Cluj-Napoca, Cluj-Napoca, Romania, 2016.

[18] R. W. Erickson and D. Maksimović, *Fundamentals of power electronics*, Second edition, Softcover reprint of the hardcover 2nd edition 2001. New York, NY: Springer Science+Business Media, LLC, 2001.

[19] **S. I. Salcu**, M. Bojan, and G. I. Fasolă, "Integrating the Behavior at Reactive Power Flow in the Model of the Single-Phase PWM Rectifier," in *Proceedings of Seventh International Congress on Information and Communication Technology*, Singapore, 2023, pp. 607–615. doi: 10.1007/978-981-19-2397-5_54.

[20] N. Norman S., *Control Systems Engineering*, 6th ed. Wiley, 2011.

[21] C. Briat, *Linear Parameter-Varying and Time-Delay Systems*, vol. 3. Berlin, Heidelberg: Springer Berlin Heidelberg, 2015. doi: 10.1007/978-3-662-44050-6.

[22] K. J. Åström and B. Wittenmark, *Adaptive Control*. Courier Corporation, 2008.

[23] C. Briat, *Linear Parameter-Varying and Time-Delay Systems*, vol. 3. Berlin, Heidelberg: Springer Berlin Heidelberg, 2015. doi: 10.1007/978-3-662-44050-6.

[24] J. Mohammadpour and C. W. Scherer, Eds., *Control of Linear Parameter Varying Systems with Applications*. Boston, MA: Springer US, 2012. doi: 10.1007/978-1-4614-1833-7.

[25] "RT Box User Manual.pdf." Accessed: Feb. 09, 2023. [Online]. Available: https://www.plexim.com/sites/default/files/rtboxmanual.pdf;

[26] "MicroDAQ E2000 datasheet.pdf." Accessed: Feb. 09, 2023. [Online]. Available: http://www.microdaq.org/products/MicroDAQ%20E2000%20datasheet.pdf;